JOURNAL OF GEOPHYSICAL RESEARCH, VOL. 98, NO. C10, PAGES 18,181–18,199, OCTOBER 15, 1993

Shorerise and Bar-Berm Profiles on Ocean Beaches

DOUGLAS L. INMAN, M. HANY S. ELWANY, AND SCOTT A. JENKINS

Center for Coastal Studies, Scripps Institution of Oceanography, La Jolla, California

A beach equilibrium model is developed that treats the outer (shorerise) portion of the profile independently from that of the inner (bar-berm) portion. The two portions are matched at the breakpoint-bar. The partitioning of the profile in this way is consistent with the different forcing modes on either side of the breakpoint. This formulation utilizes beach profile data not previously available. It is shown that both portions of the profile are well fitted by curves of the form $h = Ax^m$, where h is positive downward and x is the positive offshore coordinate. Surprisingly, the value of $m \approx 0.4$ is nearly the same for shorerise and bar-berm and does not change significantly with seasonal beach changes (summer/winter). The principal difference between seasonal profiles is that in winter (higher waves) the breakpoint-bar is deeper and farther offshore while the berm crest is displaced landward. Thus the changes in seasonal equilibria are manifested by simple, self-similar displacements of the bar-berm and shorerise curves as a consequence of changes in surf zone width and $O(1)$ variations in the factor A.

INTRODUCTION

Perhaps the single, most important concept in the field of nearshore processes is that of the equilibrium profile of beaches. In its most general sense, this concept dictates that beaches respond to wave forcing by adjusting their form to an equilibrium or constant shape attributable to a given type of incident wave. Thus the well-known seasonal changes in beach profile in response to high waves of winter and the lower waves of summer are expressions of changes in the beach form as it tends toward a seasonal equilibrium with the changing character of the prevailing waves.

An equilibrium profile must by definition be one along which the local, time-averaged, cross-shore sediment transport is everywhere zero, as are the gradients in longshore transport. However, the attributes of wave forcing that drive sediment transport and profile changes, the types of sediment transport (suspended or bedload), and the mechanics of the beach response are far from agreed upon. Does the beach profile adjust in a manner that dissipates all of the wave energy as some claim [e.g., *Keulegan and Krumbein*, 1949; *Dean*, 1977], or is there a local balance in the transport energetics that results in an equilibrium slope as claimed by others [e.g., *Inman and Bagnold*, 1963; *Bailard*, 1981; *Bailard and Inman*, 1981]; or are these concepts interrelated, and in what way? These are some of the questions addressed in this paper and a companion paper on modeling (S. A. Jenkins et al., manuscript in preparation, 1993).

Because of the importance of equilibrium profiles to beach modeling and the increased availability of beach profiles, there has been considerable recent activity in the literature [e.g., *Inman and Dolan*, 1989; *Larson and Kraus*, 1989; *Dean*, 1991]. However, the present paper is the first to consider the equilibrium profile in terms of the very real differences in forcing from deep water to the breakpoint by shoaling waves, as contrasted with that by the breaking waves and their bores in the surf zone. These two discontinuous portions of the profile are referred to here as the "shorerise" and "bar-berm" segments of the beach profile, terms introduced by *Inman and Dolan* [1989] and *Winant et al.* [1975], respectively.

The classical description of bar formation includes onshore transport outside the breakpoint and offshore transport inside, associated with the changes in forcing at the breakpoint [e.g., *Bagnold*, 1947; *Keulegan*, 1948; *Shepard*, 1950*a*; *Carter et al.*, 1973; *Lau and Travis*, 1973; *Short*, 1975 *a*, *b*; *Larson and Kraus*, 1989; *Roelvink and Stive*, 1989]. Accordingly, it is reasonable to assume that the profiles on and offshore of the breakpoint-bar respond to different forcing, and therefore should be fit by separate curves matched at the bar. However, most preceding investigations have considered the major discontinuity in profile at the breakpoint-bar as a minor aberration and have fitted single curves to the overall profile, usually omitting that portion above mean sea level (MSL) [e.g., *Bruun*, 1954; *Dean*, 1991]. Also, in part, the single curve fitting below MSL has resulted because of the absence of extensive data seaward of the breakpoint.

Fenneman [1902] introduced the concept with the statement, "There is a profile of equilibrium which water would ultimately impart, if allowed to carry its work to completion." But he goes on to define a longer-term equilibrium profile as the shape that "when once attained is maintained with some consistency." *Johnson* [1919, p. 216], says, ". . . the profile of equilibrium is maintained in as great perfection as rapidly varying (wave) conditions will permit . . ." Geologists and shoreline modelers usually use equilibrium in the sense of the longer-term, more consistent (average) profile, while coastal oceanographers and engineers mean a shorter-term profile that is in equilibrium with changing wave conditions. *Inman and Dolan* [1989] refer to the former fixed form as a "translational" profile, and the changing form as a "transient" profile which, with constant wave forcing and sufficient time, becomes an "equilibrium" profile.

The first interpretive study of profile changes and cross-shore transport on an ocean beach was that of *Shepard and LaFond* [1940], made from the Scripps Institution of Oceanography pier at La Jolla, California. The same year, *Evans* [1940] published a study of bar formation along the shores of Lake Michigan. The measurements of Shepard and LaFond clearly showed the profile response to day-by-day changes in wave conditions as well as those associated with storms and seasonal wave climate. They

Paper number 93JC00996.
0148–0227/93/93JC–00996$05.00

measured changes in sand level greater than 1.2 m in depths of 2.5 m during a 24-hour period.

Since these early studies, numerous conceptual models have been developed to explain features of the equilibrium profile and the beach response to changing wave conditions. Models purporting to explain the mechanics leading to the form of the beach profile include those developed by *Keulegan and Krumbein* [1949], *Inman and Bagnold* [1963], *Dean* [1977], *Bowen* [1980], and *Bailard* [1981]. *Keulegan and Krumbein* [1949] concluded that a shoaling solitary wave would result in a stable profile of the form $h = Ax^m$, where h is depth, A is a constant of proportionality, x is distance from shore, and the exponent m has a value of 4/7. *Inman and Bagnold* [1963] developed a model for equilibrium slopes under oscillatory motion based on the differential energy dissipation at the granular bed. *Aubrey et al.* [1980] tested the Inman and Bagnold relation using a 5-year data set of waves and beach profiles at Torrey Pines Beach. They found the model to correctly predict trends in the beach profiles but concluded that generally there was insufficient time for the beach to adjust to changing wave conditions.

Bruun [1954] made an extensive study of beach profiles along the North Sea coast of Denmark and a somewhat limited study of profiles at Mission Beach, San Diego, California. On average, he found that the relation $h = Ax^m$ held for stable configurations with values of A and m of 0.20 and 2/3 for Denmark and 0.22 and 2/3 for Mission Beach, respectively. *Dean* [1977; 1991], using profiles reported on by *Hayden et al.* [1975], found that the average beach profile along the Outer Banks of North Carolina followed the same form with values of A and m of 0.13 and 2/3, respectively. Dean's profiles, which extend from MSL to depths of about 6 m, omit the important profile changes associated with the berm as well as those seaward of 6 m depth.

Following the approach of *Keulegan and Krumbein* [1949], *Dean* [1977] considers three conditions for equilibrium due to dissipation of shallow-water linear waves. He finds that if equilibrium is associated with (1) the longshore component of radiation stress, then $m = 2/5$; (2) wave energy dissipation per unit area of the bed, then $m = 2/5$; and (3) wave energy dissipation per unit volume of the water column, then $m = 2/3$. *Bowen* [1980] studied the form of equilibrium profiles by requiring that the local transport be zero in *Bagnold*'s [1963] transport relations. Bowen found that suspended load transport in shallow water gave profiles with $m = 2/3$, provided that near-bed current consisted of an oscillatory term plus a steady current perturbation as in downwelling, upwelling and "bottom wind." However, the exponent $m = 2/5$ was found when the near-bottom current was an oscillatory term including a second-order Stokes perturbation.

Studies in large wave channels capable of reproducing near-prototype waves began with work at the Coastal Engineering Research Center, U.S. Army Corps of Engineers [*Saville*, 1957]. These studies were furthered by the work of *Kajima et al.* [1983], *Dette and Uliczka* [1987], and *Kraus and Larson* [1988]. *Larson and Kraus* [1989] developed a numerical model for beach change based largely on a comprehensive review of data from large wave channels. Their model assumes that the profile has the form $h = Ax^{2/3}$ as prescribed by *Bruun* [1954] and *Dean* [1977, 1991]. The large-scale models have added to our understanding of beaches in the vicinity of the breakpoint and berm but tell us little about the profile in deeper water.

PROCEDURE

The basic data for this study are from the 23 historic profile ranges of the San Diego region which cover the 40-year period of 1950-1989 [U.S. Army Corps of Engineers, Los Angeles District (*USACE LAD*), 1991*b*, Appendix B]. These profiles were utilized for a study of the sediment budget [*Inman and Masters*, 1991], and eight of these ranges, covering the longest period of time and extending to the greatest depths, are used here and referred to as the "basic data set" of 51 double-fitted, compound parabolic curves (Figures 1 and 2). In addition, a number of other profiles were analyzed for comparison, including Torrey Pines, which was used in previous studies of the San Diego region, and profiles from North Carolina and the Nile delta coasts, which have different wave climates and tidal ranges.

The California profiles are from a narrow-shelf coast with a spring tidal range of 1.8 m and a wave climate characterized by significant, near-breaking wave heights of $1 \le H_s$ (m) ≤ 6 and peak spectral periods of $5 \le T_p$ (s) ≤ 20 [e.g., *USACE LAD*, 1991*a*]. The Duck, North Carolina, profiles are from a wide-shelf coast with a spring tidal range of 1 m and a near-breaking wave climate characterized by $1 \le H_s$ (m) ≤ 5 and $5 \le T_p$ (s) ≤ 15 [e.g., *Coastal Data Information Program* (*CDIP*), 1992; *Stauble*, 1992]. The Nile delta profiles are from a seacoast with very gentle shelves, a tidal range less than 30 cm, and a wave climate characterized by $\frac{1}{2} \le H_s$ (m) ≤ 3 and $3 \le T_p$ (s) ≤ 8 [e.g., *Elwany et al.* 1988].

Before curve fitting, the data points from each profile were divided at the breakpoint-bar into two subsets: a bar-berm subset, extending from the berm crest to the breakpoint-bar, and a shorerise subset, extending from the breakpoint-bar seaward to depths of at least 12 m below MSL. Here we use "breakpoint-bar" to mean the bar that is commonly at or near the breakpoint of the waves, and we avoid the genetic implications of "breakpoint bar" (without the hyphen) introduced by *King and Williams* [1949] [e.g., *Bates and Jackson*, 1980]. Because a prominent breakpoint-bar is often absent from profiles in the San Diego region, in practice, the change in slope from the nearly horizontal surf zone to the more steeply sloping shorerise was used to separate the two data subsets.

A number of curve-fitting schemes were considered, including exponential, logarithmic, and parabolic, but only the latter provided good fits to the data. Accordingly, curve fitting utilized the parabolic function $h - h_0 = A(x - x_0)^m$, where x_0 and h_0 are the coordinates of the origin of the curve. When the origin of the coordinate system coincides with that of the curve, the relation reduces to

$$h = Ax^m \tag{1}$$

which is the simplest relation between depth h and distance x measured along the beach profile (Figure 2). This function reduces to a straight line when $m = 1$ and a parabola when $m = 1/2$. Parabolic curves (m positive) always pass through the origin ($x = 0$, $h = 0$) and the point $x = 1$, $h = A$. The slope β of the profile becomes

$$\tan\beta = dh/dx = Amx^{m-1}$$

so that Amx^{m-1} is the slope at any point x measured from the origin of the curve. When the logarithm of equation (1) is taken,

$$\log h = m \log x + \log A \tag{2}$$

and the parameters A and m can be readily estimated by linear regression (least squares) techniques. For convenience, we used the above logarithmic transform for fitting curves to the data, as we found there was no significant difference by least squares fitting between the logarithmic versus the real spatial domain.

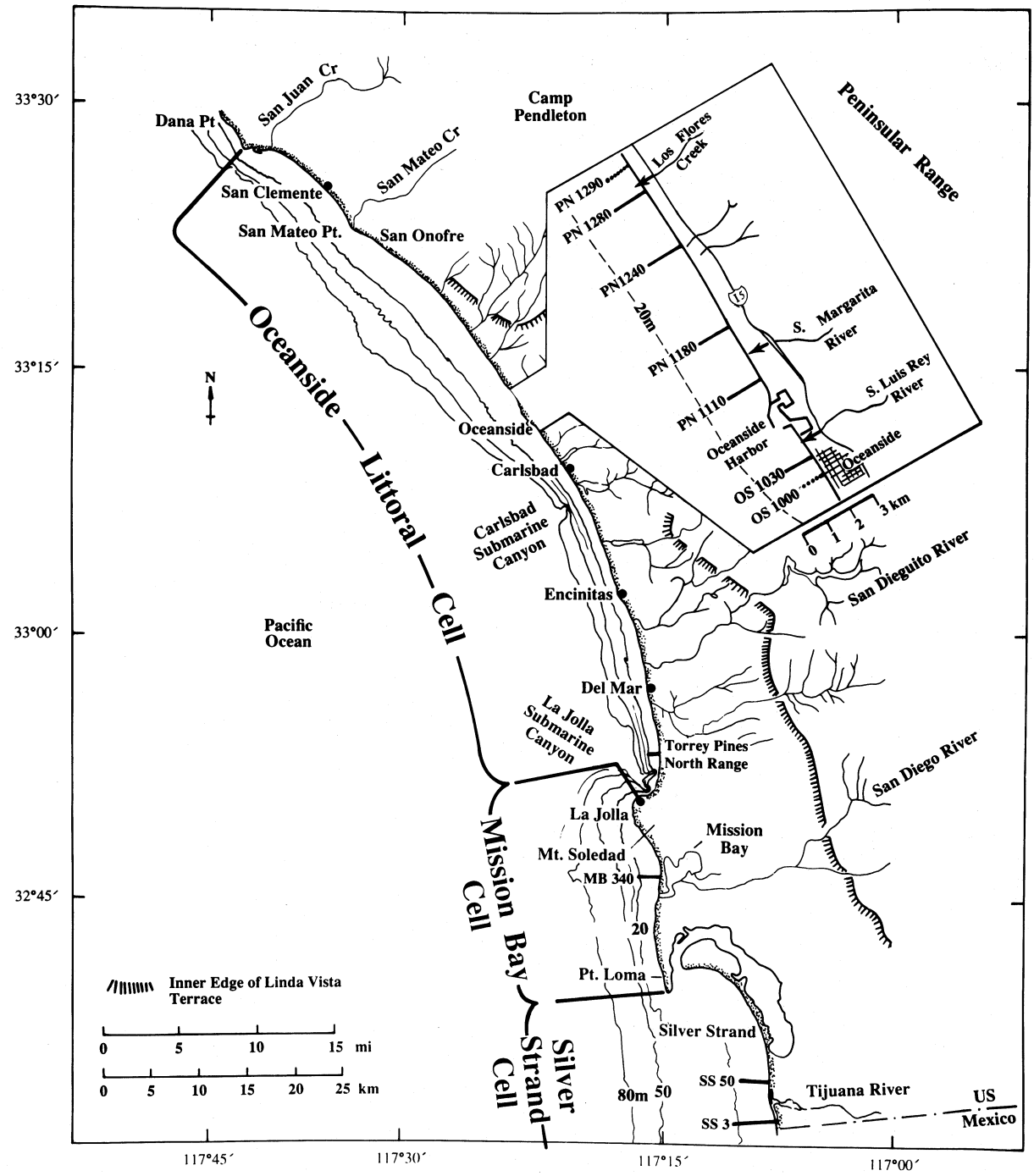

Fig. 1. Location and physiographic setting for profiles in the San Diego region. Profiles for basic data set (solid lines) and supplementary profiles for sand size (dotted lines).

The best fit origin of the bar-berm curve is at (X_1, Z_1), and that for the shorerise, at $(X_1+X_2, 0)$, as shown in Figure 2. Parabolic curves are vertical at the origin, while the maximum profile slope cannot exceed the angle of repose of the material, about 30°. Therefore it is not possible to fit a parabolic curve to a real beach when the curve's origin falls on the beach profile. Accordingly, the best fit origins for both shorerise and bar-berm curves were determined by iteration of the origin points to obtain the curve with the highest correlation coefficient. In practice, it was found that (X_1, Z_1) defined a point that on average was 1.3 m above the crest of the berm, where X_1 is the horizontal distance between the reference benchmark for the profile range and the origin of the bar-berm curve, and Z_1 is its vertical distance above MSL. The best fit origin of the shorerise curve was found to always fall on "zero" MSL at a horizontal distance X_2 from the origin of the bar-berm curve. The intersection of the bar-berm and shorerise profiles has coordinates of (X_1+X_3), Z_3. Thus X_3 is the horizontal length of the bar-berm profile, while Z_3 is approximately equal to the depth of the breakpoint-bar below MSL as shown in Figure 2.

Previous studies show that southern California beaches respond to seasonal patterns in wave forcing by attaining seasonally characteristic forms during late summer and winter [e.g., *Shepard and LaFond*, 1940; *Shepard*, 1950*b*; *Nordstrom and Inman*, 1975; *Winant et al.*, 1975; *Aubrey et al.*, 1980]. Systematic curve fitting

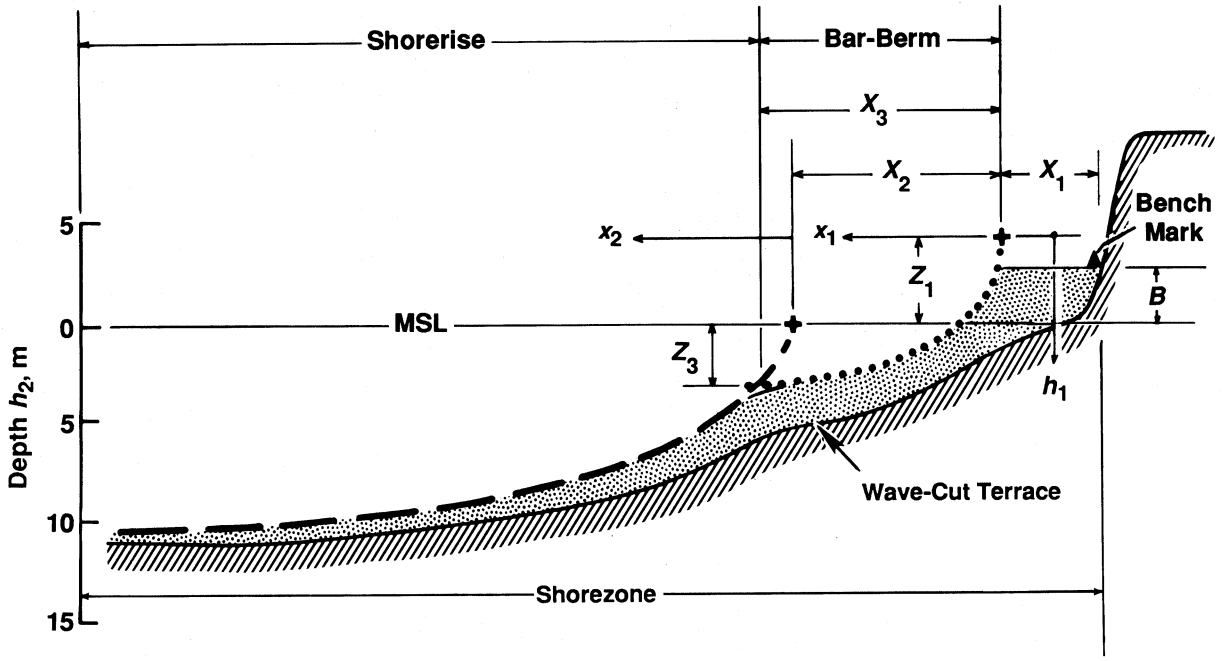

Fig. 2. Definition sketch for curve fitting. Crosses denote the origin for bar-berm (dotted) and shorerise (dashed) curves, with x coordinates, x_1, x_2, and vertical coordinates, h_1, h_2.

of basic data for all months showed that profiles measured toward the end of summer (late August, September, October) and those measured toward the end of winter (March, April) approached different but seasonally stable configurations. These seasonal equilibrium profiles are hereinafter designated as summer (S) and winter (W) profiles. Profiles measured during other months are designated as transitional (T), and the three seasonal types indicated by S, W, and T in the tables. All profiles in the basic data set that both satisfied the seasonal criterion and had continuous data from the berm crest to a depth of 12 m below MSL were analyzed. In addition, several profiles of specific interest were added to the winter listing, including profiles following the high waves of February 1952 and the intense storm of January 1988. The parameters for the individual best fit curves are listed in Table 1*a* for the basic data set and Table 1*b* for the supplementary set.

ANALYSIS

A series of comparisons were made to determine the increased accuracy of the compound parabolic curves (shorerise and bar-berm) versus a single fitted, parabolic curve. The single curve was fitted to the entire profile using the technique described above for the bar-berm (i.e., h_1 versus x_1), but, in this case, applied to the entire data set extending from the berm crest to the toe of the shorerise. It was found that the compound-fitted curves gave significantly better fits to the data (Figure 3), with rms errors in depth of about 35 cm. Comparable errors for the single fitted curves were in excess of 90 cm. The rms errors for all compound-fitted curves are listed in Tables 1*a* and 1*b*.

Basic Data Set

Since the individual bar-berm and shorerise curves are parabolic, their ensemble dynamics were first evaluated using the log-transform according to equation (2). In this form, m is the slope of the log-transform and A is the h axis intercept. The mean curves for the data sets (Figures 4*a* and 4*b*) are plotted as heavy lines, where the mean $\bar{m}$ is the simple arithmetic mean of the log slope, while the mean $\bar{A}$ is the antilogarithm of the mean h axis intercept of the log-transform. The mean data by range are listed in Tables 2*a* and 2*b* and the seasonal averages are given in Table 3.

Inspection of Figure 4 shows that the data sets for the bar-berm are somewhat more coherent than those for the shorerise. The two lowest curves for shorerise summer profiles are from range MB340 (see Figure 1) while the three higher values for winter are from SS3 (Figure 1). It is possible that the somewhat anomalous MB340 curves were influenced by beach nourishment at Mission Beach, while range SS3 has slightly coarser bar-berm sand (Table 4) which may be deposited on the winter shorerise. However, these findings were not considered sufficient reason for excluding these ranges from the data set.

The mean values of the parameters A and m for compound-fitted curves of all seasons were surprisingly similar with nearly constant values of $m \approx 0.4$ and $O(1)$ variance in A (Table 3, top). For all data in this set, the means for the bar-berm had slightly lower values of A_1 (0.78 ± 0.06) and slightly higher values of m_1 (0.41 ± 0.01) than the corresponding parameters for the shorerise with mean values of $A_2 = 1.06 \pm 0.06$ and $m_2 = 0.36 \pm 0.01$, where ± refers to the standard error for m and the antilogarithm of the log-standard error for A of the data summarized in the top part of Table 3.

Comparison of summer with winter profiles showed that both bar-berm and shorerise profiles had values of A that were lower in summer and higher in winter than the mean values for all data. Mean summer and winter values of A were 0.74 versus 0.96 for the bar-berm and 0.73 versus 1.52 for the shorerise, respectively. Conversely, the values of m were higher in summer and lower in the winter than the overall mean values. Mean summer and winter values of m were 0.41 versus 0.39 for the bar-berm and 0.42 versus 0.31 for the shorerise, respectively (Table 3, top).

TABLE 1*a*. Best Fit Parameters for Curves $h = Ax^m$ for Bar-Berm and Shorerise Profiles: Basic Data Set

Profile[a] Date	Type[b]	Bar-Berm				Compound			Shorerise			Error[c]		
		X_1	Z_1	A_1	m_1	X_3	B	Z_3	X_2	A_2	m_2	rms_1	rms_2	rms_3
						PN1280								
Oct86	S	15	4.6	0.77	0.44	263	3.3	4.4	196	0.84	0.39	0.37	0.27	0.30
Sep87	S	15	5.2	1.11	0.38	269	4.2	4.1	211	0.84	0.39	0.36	0.33	0.34
Jul82	T	0	4.9	0.80	0.42	261	4.0	3.4	227	0.98	0.35	0.35	0.33	0.34
Apr86	W	15	5.3	1.62	0.32	347	3.9	5.2	303	1.88	0.27	0.50	0.32	0.32
						PN1240								
Oct50	S	0	4.0	1.47	0.30	171	2.6	2.5	152	0.69	0.41	0.16	0.29	0.28
Oct86	S	43	4.1	1.44	0.30	178	2.4	2.4	152	0.74	0.40	0.35	0.40	0.37
Sep87	S	55	3.3	1.18	0.29	182	2.2	2.0	174	0.93	0.37	0.17	0.26	0.25
Jan72	T	0	4.7	0.77	0.42	338	2.7	4.2	319	1.94	0.26	0.29	0.22	0.24
Jul82	T	0	4.0	1.39	0.30	246	2.6	2.4	221	0.93	0.36	0.27	0.24	0.24
Feb52	W	0	4.0	0.93	0.38	361	2.5	4.7	335	2.09	0.25	0.18	0.16	0.16
Apr56	W	0	5.0	1.84	0.30	280	2.6	3.2	258	1.12	0.34	0.35	0.34	0.34
Apr86	W	0	5.6	0.76	0.45	360	2.7	5.1	319	1.89	0.27	0.52	0.18	0.28
						PN1180								
Oct86	S	0	4.6	0.65	0.45	212	3.0	2.6	198	0.99	0.37	0.21	0.14	0.20
Sep87	S	3	4.3	0.45	0.50	223	3.0	2.4	210	0.91	0.38	0.34	0.22	0.25
Jul82	T	46	2.7	0.19	0.66	216	2.4	3.3	198	1.74	0.28	0.14	0.14	0.14
Mar81	W	3	5.0	0.83	0.44	297	3.3	5.2	216	1.16	0.34	0.31	0.24	0.25
Apr86	W	3	5.0	1.15	0.36	256	3.2	3.5	232	1.14	0.35	0.20	0.23	0.22
Apr87	W	3	4.3	1.03	0.38	265	3.3	3.9	247	1.37	0.33	0.25	0.22	0.22
						PN1110								
Oct50	S	79	4.4	1.43	0.33	96	2.1	2.1	79	0.57	0.45	0.24	0.24	0.24
Oct86	S	177	3.8	0.64	0.42	162	2.3	1.6	159	1.14	0.35	0.23	0.18	0.18
Sep87	S	195	2.4	0.51	0.43	131	2.1	1.7	125	0.90	0.38	0.16	0.25	0.25
Jan72	T	55	3.1	0.50	0.48	183	2.0	3.0	166	1.08	0.36	0.18	0.30	0.29
Jul82	T	85	2.6	0.58	0.44	149	1.9	2.6	135	1.06	0.35	0.13	0.29	0.28
Jun83	T	116	1.4	0.29	0.40	189	1.2	1.0	188	0.85	0.39	0.23	0.31	0.30
Mar63	W	61	2.5	0.50	0.45	192	2.4	2.8	175	1.02	0.36	0.29	0.24	0.25
Apr87	W	153	3.8	0.56	0.46	255	3.4	3.4	244	1.63	0.30	0.39	0.21	0.25
						OS1030								
Oct59	S	0	3.1	0.56	0.45	178	2.0	2.7	152	0.70	0.41	0.32	0.14	0.17
Oct63	S	73	4.0	0.69	0.47	176	3.1	3.8	143	1.17	0.34	0.21	0.13	0.16
Oct86	S	43	3.4	0.91	0.35	181	2.5	2.2	174	1.06	0.37	0.16	0.24	0.24
Sep87	S	37	2.6	0.61	0.41	182	1.9	2.5	171	1.06	0.37	0.18	0.13	0.13

TABLE 1*a*. (continued)

Profile[a] Date	Type[b]	Bar-Berm				Compound			Shorerise			Error[c]		
		X_1	Z_1	A_1	m_1	X_3	B	Z_3	X_2	A_2	m_2	rms_1	rms_2	rms_3
						OS1030 (continued)								
Apr63	T	73	4.7	0.52	0.55	193	4.1	4.2	163	1.00	0.37	0.17	0.21	0.20
May64	T	73	5.0	1.10	0.43	91	3.5	2.6	79	1.12	0.35	0.19	0.21	0.20
Jun82	T	61	2.9	0.48	0.47	181	2.4	2.6	160	0.80	0.39	0.13	0.26	0.25
Apr86	W	31	4.7	1.19	0.35	289	2.4	3.9	233	0.70	0.43	0.29	0.31	0.29
Apr87	W	43	4.7	1.56	0.32	272	2.6	4.0	202	0.82	0.41	0.38	0.30	0.30
						MB340								
Oct86	S	0	4.0	0.68	0.41	111	2.5	0.7	105	0.23	0.60	0.26	0.33	0.30
Sep87	S	0	4.2	0.61	0.43	147	2.8	1.0	139	0.30	0.58	0.22	0.25	0.25
Apr51	W	21	3.7	0.68	0.43	211	2.7	3.1	192	0.95	0.40	0.23	0.50	0.46
Apr86	W	0	3.7	0.51	0.49	327	2.9	5.0	305	2.04	0.29	0.36	0.42	0.40
Apr87	W	0	4.9	1.43	0.32	281	2.9	3.8	244	0.80	0.43	0.39	0.22	0.27
						SS50								
Aug84	S	0	3.4	0.44	0.50	117	2.8	1.4	114	0.86	0.40	0.10	0.22	0.21
Oct86	S	0	4.3	0.52	0.48	145	3.2	1.4	136	0.48	0.47	0.24	0.41	0.39
Sep87	S	0	4.2	0.45	0.49	163	3.2	1.3	160	0.87	0.38	0.32	0.17	0.20
Jan84	T	0	3.8	1.03	0.34	155	2.8	1.9	149	0.95	0.39	0.26	0.34	0.33
Mar73	W	88	3.4	1.03	0.33	233	3.4	2.8	230	2.18	0.25	0.26	0.17	0.20
Apr86	W	0	5.2	1.37	0.34	307	2.9	4.4	294	2.31	0.25	0.46	0.18	0.30
Apr87	W	0	4.6	0.92	0.42	213	3.2	4.2	160	0.88	0.39	0.34	0.27	0.28
						SS3								
Sep87	S	67	3.8	1.23	0.31	187	2.8	2.4	167	0.54	0.50	0.22	0.81	0.77
Mar69	W	21	4.1	0.81	0.40	284	3.3	3.7	283	3.49	0.21	0.34	0.42	0.39
Apr87	W	18	4.6	0.88	0.40	289	3.3	3.9	287	3.36	0.21	0.47	0.35	0.39
Jan88	W	9	5.1	0.89	0.43	357	3.3	6.0	349	3.87	0.21	0.39	0.35	0.36

Symbols are defined in Figure 2 and in text. All distances are in meters. The source for the basic data set is *USACE LAD* [1991*b*, Appendix B]. Read "Oct86" as "October 1986."

[a]California profile locations shown in Figure 1, listed here from north to south.

[b]Types are as follows: S, summer (late August to October); T, transitional; W, winter (March, April)

[c]Root-mean-square error: rms = $[\Sigma (h-h')^2/n]^{1/2}$, where h and h' are the measured and curve-fitted depths, respectively; subscripts 1, 2 and 3 indicate bar-berm, shorerise, and compound (whole) profiles, respectively.

TABLE 1*b*. Best Fit Parameters for Curves $h = Ax^m$ for Bar-Berm and Shorerise Profiles: Supplementary Data Set

Profile Date	Type[a]	Bar-Berm				Compound			Shorerise			Error[b]		
		X_1	Z_1	A_1	m_1	X_3	B	Z_3	X_2	A_2	m_2	rms_1	rms_2	rms_3
Torrey Pines (North Range)														
Oct72	S	15	2.6	0.38	0.50	156	2.2	1.7	146	0.24	0.62	0.21	0.44	0.37
Nov72	T	6	3.4	0.37	0.53	172	2.5	2.3	148	0.41	0.54	0.17	0.60	0.40
Apr73	W	24	3.7	0.40	0.53	271	2.7	4.1	218	0.52	0.52	0.51	1.14	0.83
Duck, North Carolina (Range 63)														
Aug85	S[c]	65	6.4	1.62	0.34	166	5.3	2.5	113	0.70	0.36	0.50	0.38	0.43
Aug85	S[d]	65	6.6	1.54	0.31	360	5.3	4.8	305	1.60	0.26	0.49	0.17	0.38
Mar85	W[c]	65	6.3	1.70	0.33	188	5.3	2.6	117	0.62	0.38	0.46	0.36	0.40
Mar85	W[d]	65	6.4	3.10	0.23	335	5.3	4.5	300	1.62	0.25	0.49	0.19	0.39
Profile 6/16 Nile Delta, Egypt														
Nov 76	S[e]	37	3.0	0.24	0.32	280	2.0	2.0	234	0.64	0.49	0.37	0.33	0.34
Nov 86	S[e]	50	2.4	0.70	0.40	40	2.0	0.7	32	0.21	0.48	0.15	0.27	0.24

Symbols are defined in Figure 2 and text. All distances are in meters. Sources for the supplementary data set are as follows: Torrey Pines profiles, *Nordstrom and Inman* [1975]; Duck, North Carolina, profiles, *Stauble* [1992], profiles of August 21, 1985, and March 15, 1985; Nile delta coast profiles, *Inman et al.* [1992].

[a]Types are as follows: S, summer (late August to October); T, transitional; W, winter (March, April).

[b]Root-mean-square error: $rms = [\Sigma (h-h')^2/n]^{1/2}$, where h and h' are the measured and curve-fitted depths, respectively; subscripts 1, 2 and 3 indicate bar-berm, shorerise, and compound (whole) profiles, respectively.

[c]Bar-berm and shorerise data sets divided at inner bar.

[d]Bar-berm and shorerise data sets divided at outer (second) bar.

[e]End of summer profiles (S) on the Nile delta are surveyed in November.

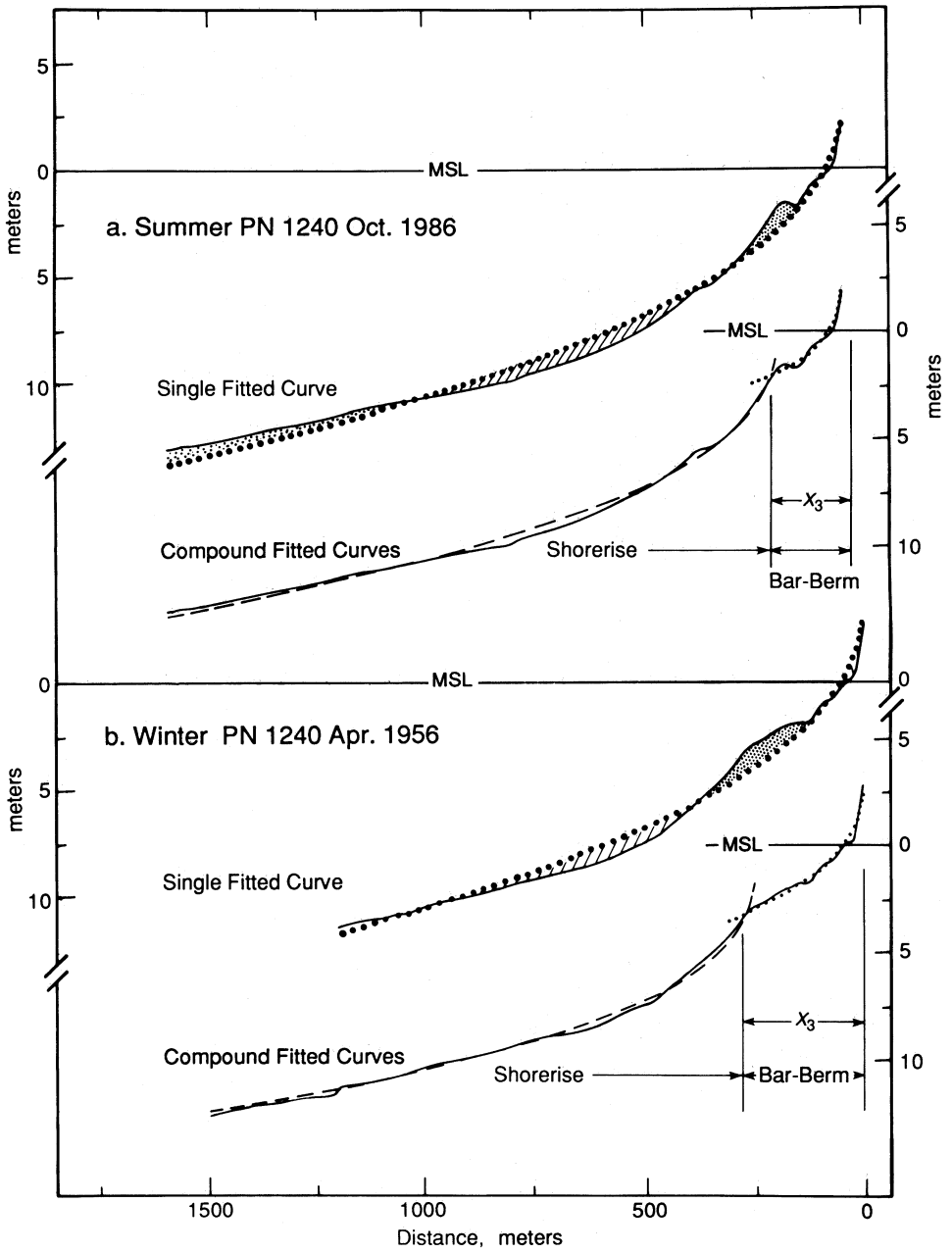

Fig. 3. Comparison of (*a*) summer and (*b*) winter measured profiles (solid line) with single-fitted curves (heavy dot) and compound-fitted curves (light dash and dot).

The basic data set includes profiles from three separate littoral cells with different sediment sources, shelf widths, wave intensities and distances from coastal structures. Accordingly, for purposes of comparison, three ranges in the vicinity of Oceanside, California, were selected that were distant from structures (>2 km) and had slightly higher waves than the mean for the basic data set. The location of these ranges (PN1280, PN1240, OS1030) are shown in Figure 1 and their mean values summarized separately in the bottom part of Table 3. Comparison of the top and bottom sections of Table 3 shows that the basic data and subset have the same trends, although the Oceanside subset, which is exposed to higher waves, has deeper bars (larger Z_3) and slightly lower values of m, indicating greater curvature.

Responses of Seasonal Equilibria

The most consistent changes between summer and winter are in the measures of surf zone width X_3 and the depth to the bar as given by the intersection of the bar-berm and shorerise curves at Z_3. For the basic data set, the overall mean summer and winter values of X_3 are 178 m and 283 m, while those for Z_3 are 2.3 m and 4.0 m, respectively (Table 3, top). Also, the summer berm, on average, as measured by X_1, is 17 m wider in summer than in winter, while the height of the berm crest B is 30 cm lower in summer than in winter. The height above the berm crest of the best fit origin for the bar-berm is $Z_1 - B$, which has an overall mean value of 1.3 ± 0.08 m. Its mean summer value is 1.2 ±

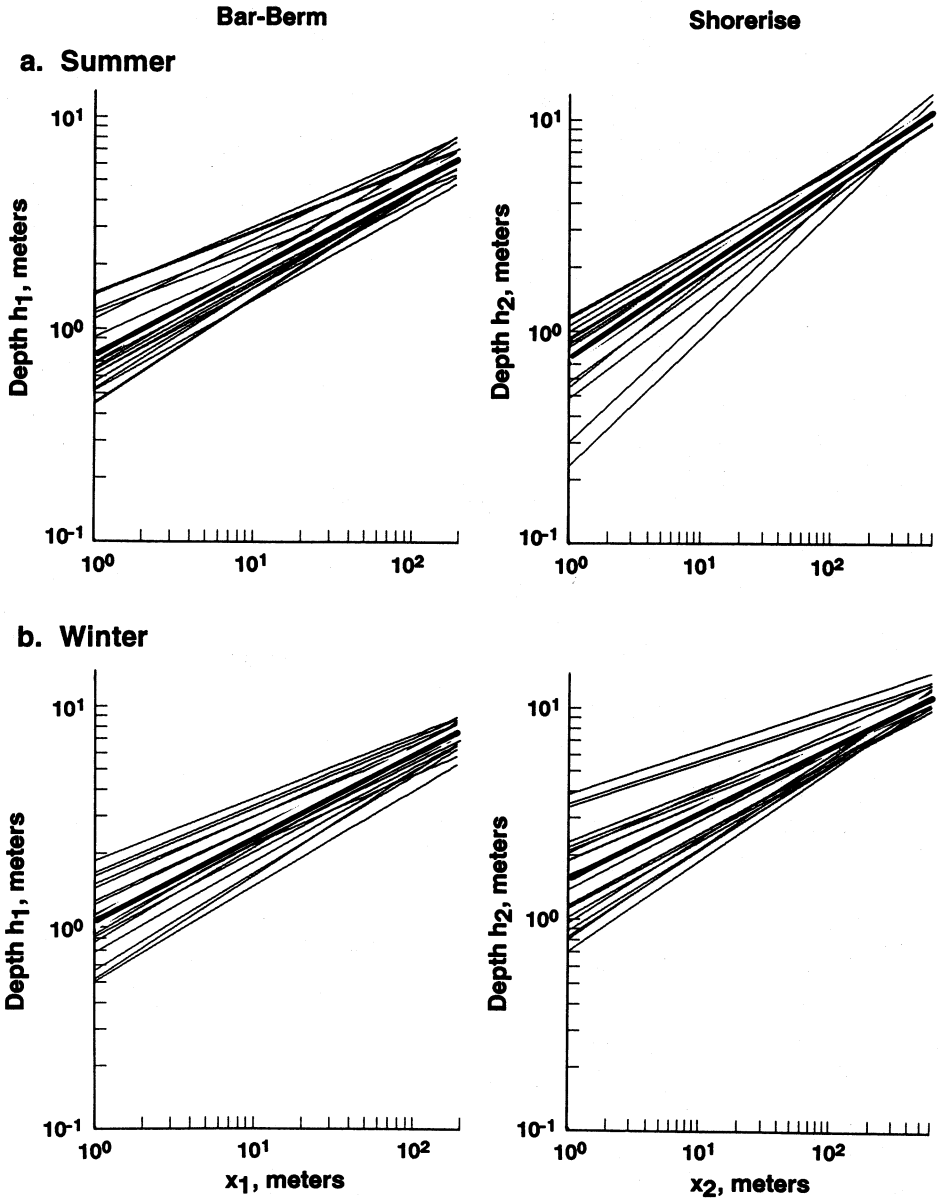

Fig. 4. Fitted, compound parabolic curves plotted on log-log scales for (*a*) summer and (*b*) winter. Individual profiles (light lines) are from data in Table 1*a*, while the seasonal mean profile (heavy line) is from the top section of Table 3. Note that 180° rotation places this figure in directional agreement with the coordinates of Figures 2, 5, etc.

0.09 m, and its winter value is 1.7 ± 0.13 m, where ± refers to the standard error.

It was found that the rms errors between individual surveys and the seasonal (summer/winter) mean parameters (Tables 2*a* and 2*b*) were not significantly greater than those for the individual surveys versus their own best fit parameters (Tables 1*a* and 1*b*). For example, using the most populous Oceanside ranges (PN1240, PN1180, OS1030), the average rms errors in meters for the nine summer surveys were 0.33, 0.39, and 0.38 for the bar-berm, shorerise, and whole profile, respectively. Similarly, the average errors for the eight winter profiles were 0.39, 0.34, and 0.35. This suggests that the summer/winter profiles as defined by the value of their mean parameters (Tables 2*a* and 2*b*) have year-to-year stability.

Comparison of summer and winter profiles, using the mean values listed in Table 3, gives reasonable values of the seasonal volume changes associated with these beaches. Seasonal profiles are shown in Figures 5*a* and 5*b*, where, for purposes of comparison, the origins of the two curves are normalized by setting the winter origin of the bar-berm equal to zero ($\bar{X}_{1W} = 0$), and the summer origin equal to the difference $\Delta\bar{X}_1 = \bar{X}_{1S} - \bar{X}_{1W}$. For the two cases shown in Figures 5*a* and 5*b*, the summer to winter seasonal volume changes are a bar-berm erosion of 93 m^3/m with a shorerise accretion of 84 m^3/m for the means of the basic data set, and changes of 92 m^3/m and 102 m^3/m, respectively, for the means of the selected Oceanside subset. The seasonal changes in bar-berm versus shorerise are approximately equal (within 10%), as they should be, and their magnitudes are in agreement with previous estimates that give the seasonal changes of these beaches as about 92 m^3/m [*Nordstrom and Inman*, 1975; *Inman*, 1987].

The above findings show that the seasonal profile changes do not involve significant changes in the fitted parameter *m* of the

TABLE 2*a*. Mean Best Fit Parameters by Profile: Basic Data Set

		Bar-Berm				Compound			Shorerise		
Number[a]	Type	$\bar{X}_1$	$\bar{Z}_1$	$\bar{A}_1$	$\bar{m}_1$	$\bar{X}_3$	$\bar{B}$	$\bar{Z}_3$	$\bar{X}_2$	$\bar{A}_2$	$\bar{m}_2$
					PN1280						
2	S	15	4.9	0.92	0.41	266	3.8	4.3	204	0.84	0.39
1	T	0	4.9	0.80	0.42	261	4.0	3.4	227	0.98	0.35
1	W	15	5.3	1.62	0.32	347	3.9	5.2	303	1.88	0.27
4	all	11	5.0	1.03	0.39	285	3.9	4.3	234	1.07	0.35
					PN1240						
3	S	33	3.8	1.36	0.30	177	2.4	2.3	159	0.78	0.39
2	T	0	4.4	1.03	0.36	292	2.7	3.3	270	1.34	0.31
3	W	0	4.9	1.09	0.38	334	2.6	4.3	304	1.64	0.29
8	all	12	4.3	1.17	0.34	265	2.5	3.3	241	1.18	0.33
					PN1180						
2	S	2	4.5	0.54	0.48	218	3.0	2.5	204	0.95	0.38
1	T	46	2.7	0.19	0.66	216	2.4	3.3	198	1.74	0.28
3	W	3	4.8	0.99	0.39	273	3.3	4.2	232	1.22	0.34
6	all	10	4.3	0.62	0.47	245	3.0	3.5	217	1.19	0.34
					PN1110						
3	S	150	3.4	0.78	0.39	130	2.2	1.8	121	0.84	0.39
3	T	85	2.4	0.44	0.44	174	1.7	2.2	163	0.99	0.37
2	W	107	3.2	0.53	0.46	224	2.9	3.1	210	1.29	0.33
8	all	115	3.0	0.57	0.43	170	2.2	2.3	159	0.99	0.37
					OS1030						
4	S	38	3.3	0.68	0.42	179	2.4	2.8	160	0.98	0.37
3	T	69	4.2	0.65	0.48	155	3.3	3.1	134	0.96	0.37
2	W	37	4.7	1.36	0.34	281	2.5	4.0	218	0.76	0.42
9	all	48	3.9	0.78	0.42	194	2.7	3.2	164	0.92	0.38
					MB340						
2	S	0	4.1	0.64	0.42	129	2.7	0.9	122	0.26	0.59
3	W	7	4.1	0.79	0.41	273	2.8	4.0	247	1.16	0.37
5	all	4	4.1	0.73	0.42	215	2.8	2.7	197	0.64	0.46
					SS50						
3	S	0	4.0	0.47	0.49	142	3.1	1.4	137	0.71	0.42
1	T	0	3.8	1.03	0.34	155	2.8	1.9	149	0.95	0.39
3	W	29	4.4	1.09	0.36	251	3.2	3.8	288	1.64	0.30
7	all	13	4.1	0.75	0.41	190	3.1	2.5	178	1.06	0.36
					SS3						
1	S	67	3.8	1.23	0.31	187	2.8	2.4	167	0.54	0.50
3	W	16	4.6	0.86	0.41	310	3.3	4.5	306	3.57	0.21
4	all	29	4.4	0.94	0.39	279	3.2	4.0	272	2.22	0.28

Values are simple arithmetic means of individual data listed in Table 1 except for $\bar{A}$, which is the antilogarithm of the mean h axis intercept of the log-transform.

[a]Number of surveys averaged.

curves. Rather, the nature of the seasonal changes takes the form of simple translations of the origins of the bar-berm and shorerise curves involving adjustments in X_1 and X_2 with small corrections to the parameter A. The summer to winter change is manifested by the displacement of the bar-berm curve to an onshore position, accompanied by an offshore displacement of the shorerise curve. In fact, it was found that the summer to winter to summer changes can be reproduced approximately by simple, self-similar displacement of the two curves, keeping the erosional volume (hatched) under the surf zone equal to the accretional volume (stippled) on the shorerise as suggested by the data comparisons in Figures 5*a* and 5*b*.

Translational Profiles

The data confirm that during periods of consistent seasonal wave climate, the cross-shore transports of the seasonal, reversible, equilibrium responses to summer and winter waves are contained within the shore zone, which includes the shorerise and bar-berm profiles (compare Figures 2 and 5). The seasonal changes extend seaward to the toe of the shorerise where the profiles of summer and winter equilibria merge asymptotically at the closure depth h_c (inset, Figure 6). They extend onshore to the closure berm height at the crest of the winter berm which has an elevation B_c above MSL. The total vertical extent of the seasonal changes is $Z_c = h_c + B_c$, referred to here as the closure interval. The closure interval Z_c is an essential parameter in shoreline modeling as it is numerically equal to the volume-equivalent factor q' (m^3/m^2) relating the volume eroded or accreted to the area of shoreline change, $Z_c \equiv q'$ [e.g., *Inman and Dolan*, 1989, equations 3.1b, 7.2]. This relation holds for a translational profile which is a fixed-form, moving flux-surface that participates in the shoreline change [e.g., *LeMéhauté and Soldate*, 1977, 1978; *Inman and Dolan*, 1989].

The seasonal profile changes discussed above are superimposed

TABLE 2*b*. Mean Best Fit Parameters by Profile: Supplementary Data Set

Number[a]	Type	Bar-Berm $\bar{X}_1$	$\bar{Z}_1$	$\bar{A}_1$	$\bar{m}_1$	Compound $\bar{X}_3$	$\bar{B}$	$\bar{Z}_3$	Shorerise $\bar{X}_2$	$\bar{A}_2$	$\bar{m}_2$
					Torrey Pines						
1	S	15	2.6	0.38	0.50	156	2.2	1.7	146	0.24	0.62
1	T	6	3.4	0.37	0.53	172	2.5	2.3	148	0.41	0.54
1	W	24	3.7	0.40	0.53	271	2.7	4.1	218	0.52	0.52
3	all	15	3.2	0.38	0.52	200	2.5	2.7	171	0.37	0.56
					Duck, North Carolina (Range 62)						
1	S[b]	65	6.4	1.62	0.34	166	5.3	2.5	113	0.70	0.36
1	W[b]	65	6.3	1.70	0.33	188	5.3	2.6	117	0.62	0.38
2	all[b]	65	6.4	1.66	0.34	177	5.3	2.6	115	0.66	0.37
1	S[c]	65	6.6	1.54	0.31	360	5.3	4.8	305	1.60	0.26
1	W[c]	65	6.4	3.10	0.23	335	5.3	4.5	300	1.62	0.25
2	all[c]	65	6.5	2.32	0.27	348	5.3	4.6	302	1.61	0.26
					Profile 6/16.0 Nile Delta, Egypt						
2	S	44	2.7	0.47	0.36	160	1.8	1.4	133	0.49	0.49
2	all	44	2.7	0.47	0.36	160	1.8	1.4	133	0.49	0.49

Values are simple arithmetic means of individual data listed in Table 1 except for $\bar{A}$, which is the antilogarithm of the mean h axis intercept of the log-transform.

[a]Number of surveys averaged.

[b]Bar-berm and shorerise data sets divided at inner bar.

[c]Bar-berm and shorerise data sets divided at outer (second) bar.

on any longer-term changes in shoreline accretion or erosion. Accordingly, it seems reasonable that the translational profile required for modeling shoreline change should take the form of the mean of the summer and winter equilibrium profiles as suggested by *Inman and Dolan* [1989]. Such a profile, based on the seasonal mean profiles for the basic data set (Table 1*a*; Figure 5*a*), is plotted in Figure 6 together with the seasonal profiles upon which it is based. The origins of the translational profile are midway between those of the seasonal profiles, and the curves have the form $A_{1T} = 0.84$, $m_{1T} = 0.40$, and $A_{2T} = 1.10$, $m_{2T} = 0.36$, as listed in Table 3.

The 40 years of record covered by the basic data set show that there are relatively long periods of a decade or so of uniform wave climate during which the seasonal cross-shore changes are all contained within the shore zone. For these periods, the data range for the closure berm height was $3 \le B_c$ (m) < 5, and the range for the depth of closure was $6.5 \le h_c$ (m) ≤ 10 resulting in closure intervals of $10 \le Z_c$ (m) ≤ 14. The closure interval and associated closure depth and berm height are clearly illustrated when the variations in depth are plotted versus depth [e.g., *Kraus and Harikai*, 1983]. Figure 7 shows a plot of the standard deviation in depth for the nine surveys taken during a 6-year period of ordinary, seasonal wave climate on range PN1240. It is apparent that the closure berm height and depth are approximately 4.5 m and 6.5 m, respectively, giving a closure interval of 11 m. The mean standard deviation was about 10 cm for depths greater than 6.5 m, which is less than the error of profile measurement, indicating no profile change at these depths.

TABLE 3. Mean Best Fit Parameters by Season

Type	Number	Bar-Berm $\bar{X}_1$	$\bar{Z}_1$	$\bar{A}_1$	$\bar{m}_1$	Compound $\bar{X}_3$	$\bar{B}$	$\bar{Z}_3$	Shorerise $\bar{X}_2$	$\bar{A}_2$	$\bar{m}_2$
					Basic Data Set						
S	20	40	3.9	0.74	0.41	178	2.8	2.3	156	0.73	0.42
T	11	46	3.6	0.60	0.45	200	2.8	2.8	182	1.09	0.35
W	20	23	4.5	0.96	0.39	283	3.1	4.0	255	1.52	0.31
all	51	35	4.1	0.78	0.41	223	2.9	3.1	200	1.06	0.36
Transl.[a]	40	32	4.2	0.84	0.40	230	3.0	3.2	206	1.10	0.36
					Selected Oceanside Profiles[b]						
S	9	31	3.8	0.91	0.38	198	2.7	3.0	174	0.88	0.38
T	6	35	4.4	0.79	0.43	218	3.1	3.2	195	1.08	0.34
W	6	15	4.9	1.26	0.35	318	2.8	4.5	275	1.30	0.33
all	21	28	4.2	0.96	0.39	238	2.9	3.4	208	1.04	0.35

Values are simple arithmetic means of individual data listed in Table 1*a* except for $\bar{A}$, which is the antilogarithm of the mean h axis intercept of the log-transform.

[a]Translational profile from the mean summer (S) and winter (W) profiles in the basic data set.

[b]Mean for profiles PN1280, PN1240, and OS1030.

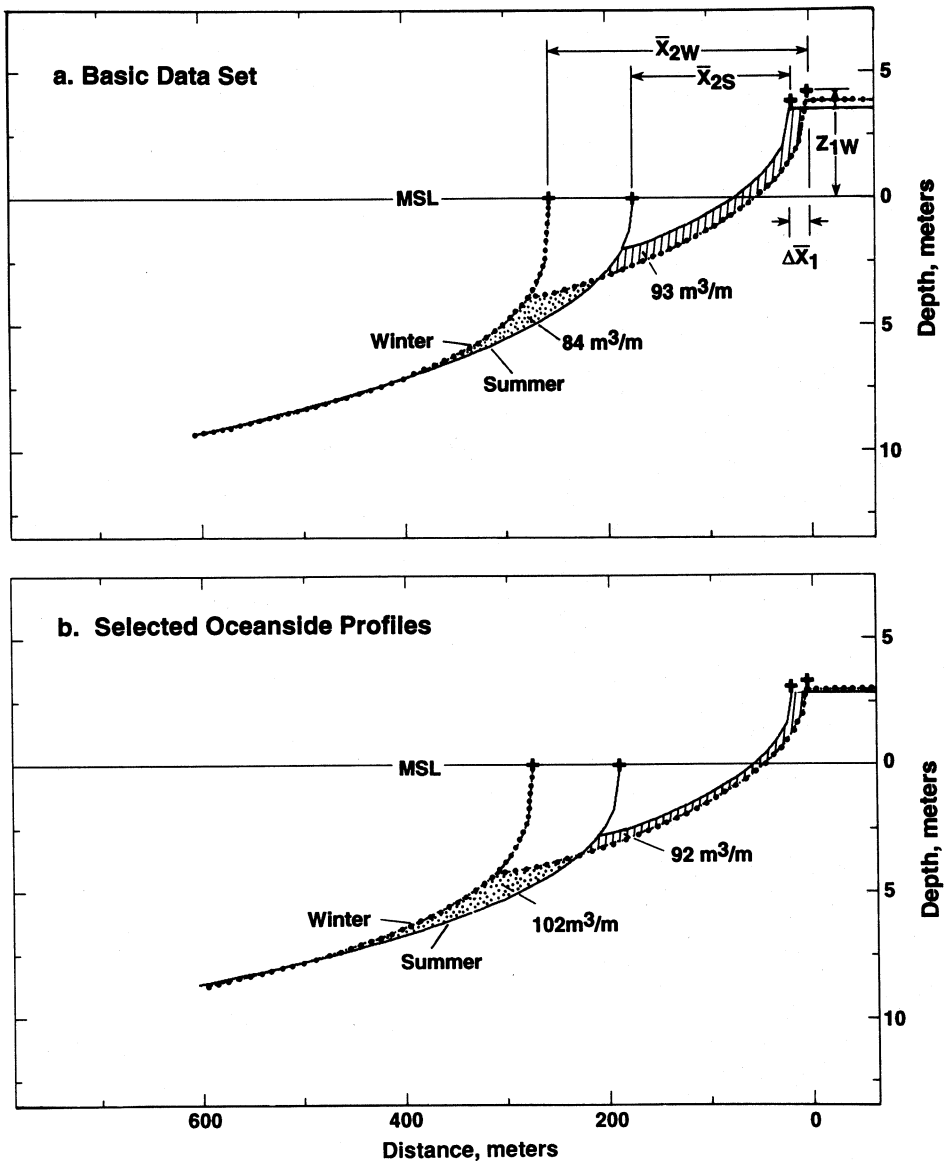

Fig. 5. Seasonal beach changes illustrated by (*a*) comparison of mean summer and winter equilibrium profiles for the basic data set (Table 3, top) and (*b*) for the Oceanside subset (Table 3, bottom).

However, it was found that winters of consistent, intense wave energy, such as that associated with the cluster storms of 1982-1983, resulted in absence of closure to the deepest depths surveyed, approximately 15 m below MSL. A graph of standard deviation in depth for the same range as Figure 7, but including surveys before and after the cluster storms of 1982-1983, is shown in Figure 8. The graph is bimodal with a minimum near the previous depth of closure, but with significant deviations in depth continuing to the greatest depths measured. This phenomenon is probably associated with the disequilibrium conditions of transient profiles.

Application of translational profiles to shoreline modeling requires verification of the existence of a closure depth during the period of study (e.g., compare Figures 7 and 8). Along the Nile delta [*Inman et al.*, 1992] it was found that accretion waves [*Inman*, 1987] associated with onshore migrating sand blankets prevented profile closure in the lee of promontories. Also, both profile studies at Duck, North Carolina [*Howd and Birkemeier*, 1987, Figure 9; *Stauble*, 1992, Figure 9], show an absence of closure over the study periods of 3 1/2 years and 18 months, respectively.

Disequilibria Responses

There are certain extreme conditions that produce more rapid changes than usual and others in which transient profiles remain in a state of disequilibria for prolonged periods. Discussion of several of these special conditions is useful in the context of profile development.

Because of its inertia, a beach requires time to achieve equilibrium for a given set of wave conditions. Model experiments with breaker heights of 10 cm show that the time to equilibrium is O(20 hours) [e.g., *Keulegan*, 1948], while for breaker height of 1 to 2 m in large wave tanks the time to equilibrium is O(100 hours) [*Larson and Kraus*, 1989]. Accordingly, complete equilibrium of the entire profile is rarely achieved in the field because wave type

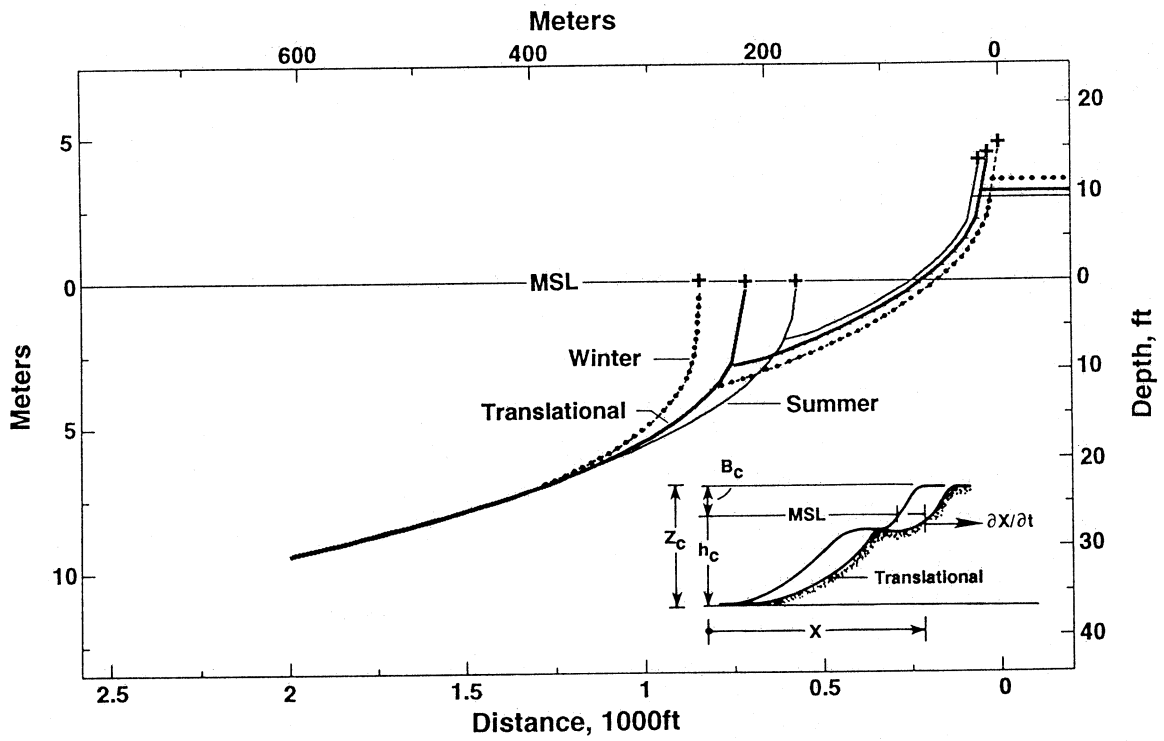

Fig. 6. Translational profile calculated from mean summer and winter equilibrium profiles of basic data set. Parameters are listed in the top section of Table 3. The inset shows the relation to the closure interval.

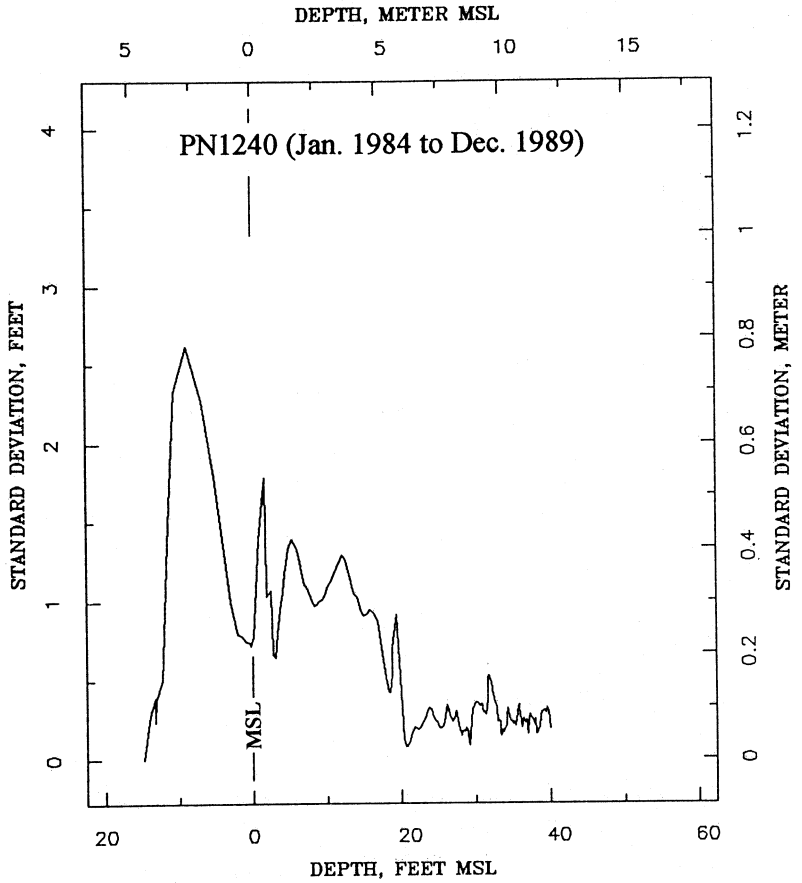

Fig. 7. Closure interval for the period January 1984 to December 1989 on range PN1240. Data are based on nine surveys with about 300 data points each. Depth of closure is approximately 6 m MSL as shown by the reduction in standard deviation of the depth changes to approximately 10 cm.

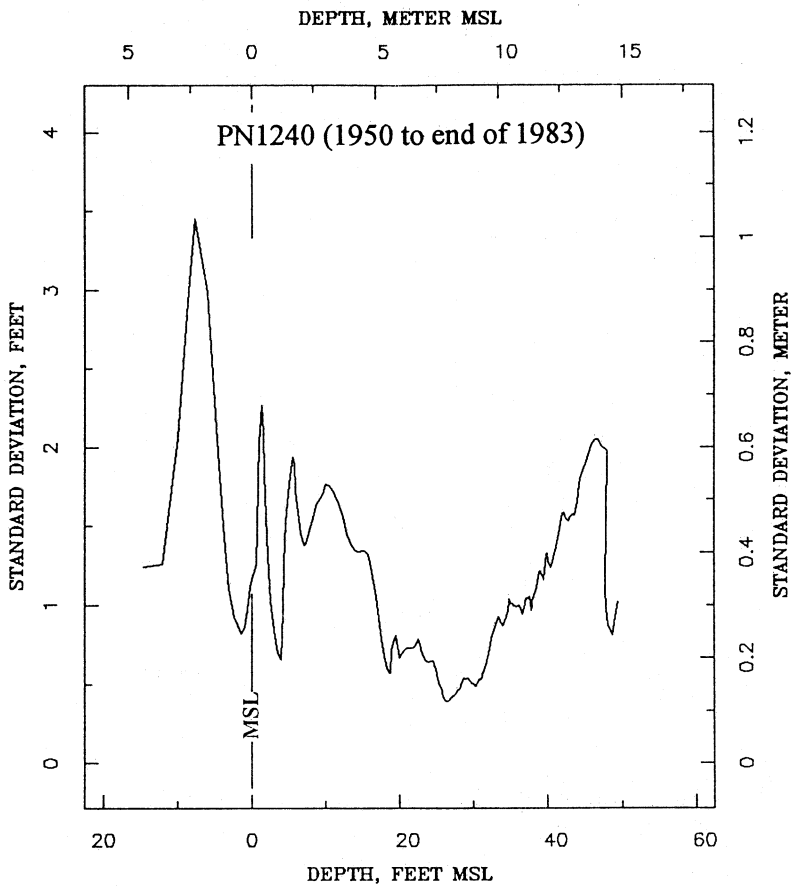

Fig. 8. Bimodal distribution of standard deviation of depth change indicating a lack of closure for this period. Data are based on seven surveys with about 300 data points each.

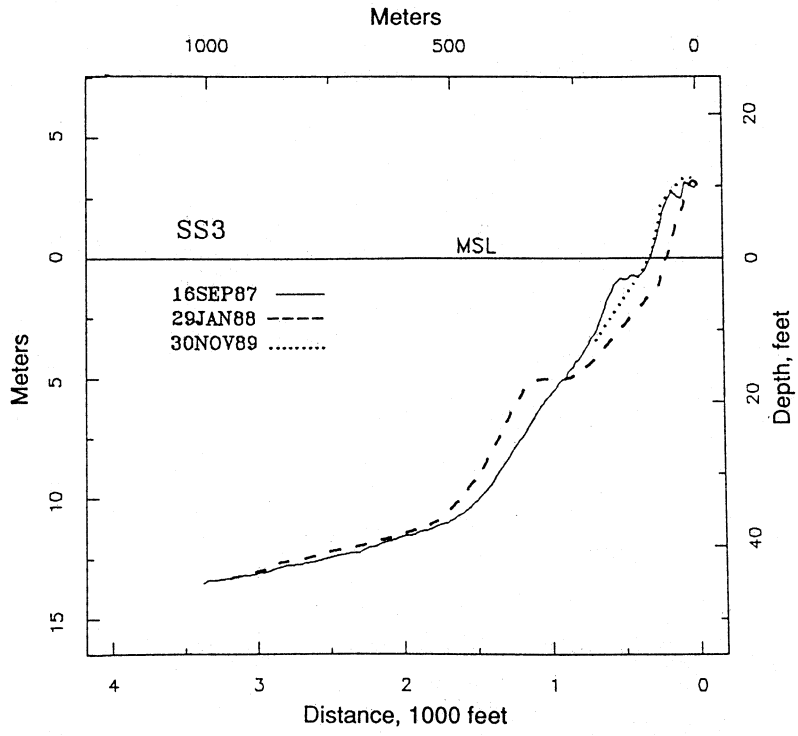

Fig. 9. Winter equilibrium profile (dashed line) produced by the storm of January 17-18, 1988.

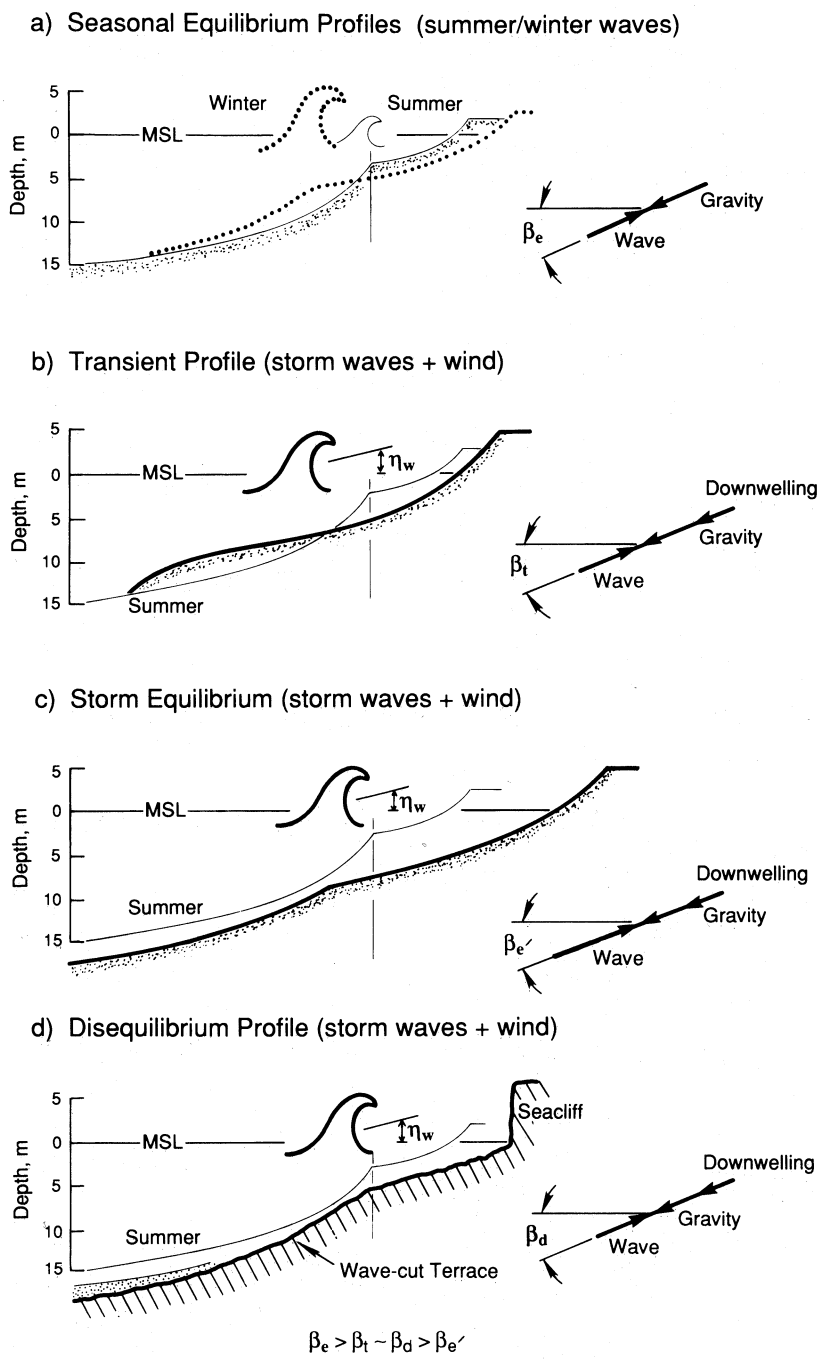

Fig. 10. Schematic diagram showing equilibrium and disequilibrium profiles and their suggested stress balance. The summer equilibrium profile (Figure 10*a*) is shown as a reference position in Figures 10*b*, 10*c*, and 10*d*.

and water level are continuously varying. However, the basic data set for the San Diego region shows that beaches attain typical seasonal profiles by the end of summer, usually late August-October, and by the end of winter, usually March-April. Profiles at times between these typical summer and winter profiles are usually transient forms in the process of transition between seasonal profiles.

However, intense storms can induce changes from summer to winter profiles in a few hours. For example, the storm of January 17-18, 1988, produced the largest waves ever measured off the coast of southern California. This storm had deepwater wave heights of 10 m, peak spectral energy in the 14- to 17-s band, and a duration of about 10 to 14 hours [*O'Reilly*, 1989; *Strange et al.*, 1989]. This one storm effectively changed the summer profile of September 1987 to the winter profile of January 29, 1988, as illustrated by Figure 9. Note that apparently no material was lost from the shore zone and that, by the succeeding survey, the profile had returned to its summer configuration. The fitted curves for profiles resulting from this storm showed typical winter values of A and m, differing from other winter profiles only in the width of the surf zone X_3 and in the depth to the breakpoint-bar Z_3 (compare Figure 9 and profile SS3 in Table 1*a*).

In contrast to the winter equilibrium profile produced by the storm of January, 1988, the cluster storms of the winter of 1982-

1983 produced erosion of the bar-berm down to the underlying country rock and downwelling of sediment from the shore zone onto the shelf. The downwelling produced a permanent deepening of the profile from the toe of the shorerise (about 10 m below MSL) to the deepest surveyed depth of approximately 15 m below MSL. Although the January 1988 storm had the highest waves ever measured, it was the only large storm of that year. The winter of 1982-1983 was an El Niño-Southern Oscillation (ENSO) event that raised sea level at San Diego over 20 cm and contained numerous cluster storms. The storms, with their accompanying strong onshore winds, occurred approximately every 3 to 5 days, and, although none had waves as high as the January 1988 storm, many were nearly as high. For example, 4 out of the 17 highest-wave storm events of this century occurred during the single winter of 1982-1983 [*Inman and Masters*, 1991, Table 9-8].

The systematic adjustments of the profile to summer and winter equilibria raise the question of why the profiles during cluster storm winters do not adjust to some form of storm equilibrium (compare Figures 10*a*, 10*b*, and 10*c*). It appears that the absence of storm equilibria along the cliffed coast of California results from an insufficient amount of sand covering the wave-cut terraces of country rock (Figure 2). In the San Diego region the thickness of this veneer of sand averages about 2.3 m under the summer bar-berm and about 1.2 m under the shorerise [*Inman and Masters*, 1991, Figure 9-9]. Accordingly, there is insufficient sand under the bar-berm and insufficient distance between the breakpoint of the waves and the seacliffs to permit the development of a storm equilibrium profile. Rather, when the beach erodes down to the wave-cut terrace, a rigid platform, steeper than that permissible for storm equilibria, is introduced (Figure 10*d*).

Relation to Sand Size

The slope of the beach face increases with increasing sand size on southern California beaches [*Inman*, 1953]. Also, these beaches have a moderate seasonal variation in sand size on the beach face and in the surf zone, with somewhat less variability on the shorerise. Sand from the beach face was best sorted and most constant in size, while that from the surf zone was most variable in size, with significantly coarser material in winter. Beach face samples were taken from a "reference level" which, for the San Diego region, is about 1.5 to 2 m above MSL. This well-known dependence of beach face slope on sediment size [e.g., *Bascom*, 1951; *Wiegel*, 1964, p. 359] suggests that A in equation (1) should vary with sand size. Using single-curve fitting, *Dean* [1977] shows an inverse relation between A and m; and when $m = 2/3$ is held constant, A is proportional to sand size [*Dean*, 1991]. Unfortunately, sediment size for our basic data set is too sparse to permit comparison of sediment size with the parameters from individual surveys or with season. Also, the range of sand size within the basic data set was insufficient to determine a dependence of A or m on sand size. Accordingly, the data set was

TABLE 4. Sand Size Versus Depth

Referenced Profiles[a]			Data Source[b]	MSL Depth				
Curve-Fitted	Sand-Sampled	Distance, km		+1.5 m to +2 m	0	- 4 m	-7 m	-9 m
			Basic Data Set					
PN1280	PN1290	1.1 N	1	360	640	110	90	
			2	370	575	110	95	
			3	385	395	120		
PN1240	→	0	3	410	200	90	125	
PN1110	→	0	1	220	200	180	160	
			2	210	190	175	145	
			3	240	225	195	120	pebbles
OS1030	OS1000	0.8 S	1	280	180	125	120	
			2	290	160	135	110	
			3		125	135	90	75
MB340	→	0	3	225	205	260	125	
SS50	SS70	2.0 N	3	265	260	190	135	
SS3	SS35	3.0 N	1	380		190	120	
			2	365		175	105	
			3	290	285	165	130	
			Supplementary Data					
Torrey Pines North Range	→	0	4	180		190	125	100
			5	230		220	110	95
Duck, Range 62	→	0	6S	420[c]	410	145	120	
			6W	440[c]	380	160	115	
Nile Range 6/16	→	0	7	250				

[a]Curve-fitted profile referenced to sand-sampled profile, which is distance in kilometers north (N) or south (S) of curve-fitted profile.

[b]Data sources for size analysis are as follows: (1) Median diameter in microns (μm) sampled October 1983 to January 1984, *USACE LAD* [1984]; (2) Mean diameter (μm) sampled October 1983 to January 1984, reanalyzed in *USACE LAD* [1985, Table 3]; (3) Mean diameter (μm) sampled February 1984 to June 1984, *USACE LAD* [1985, Table 4]; (4) Median diameter (μm) sampled July 1973, *Nordstrom and Inman* [1975]; (5) Median diameter (μm) sampled February 1974, *Nordstrom and Inman* [1975], "beach face" sample 1.5-2.0 m above MSL; (6) *Stauble* [1992]; and (7) *Inman et al.*, [1992].

[c]Composite of beach face samples.

extended to include the supplementary profiles listed in Table 2*b*. The available sand sizes for the combined data set are listed in Table 4, including beach face samples (0-2 m above MSL) as well as those from the inner portion of the shorerise (4 and 7 m below MSL). Mean values of A_1, m_1 and the product A_1m_1 from Tables 2*a* and 2*b* for bar-berm profiles are plotted versus the beach face sand diameter in Figure 11.

Even from this small data set it is apparent that the values of A_1 for the bar-berm profiles vary with the size of the sand on the beach face. The sand size ranges in diameter from approximately 200 to 440 μm. For this increase in size the value of A_1 increases from about 0.4 to 1.7; m_1 decreases from about 0.5 to 0.34, while

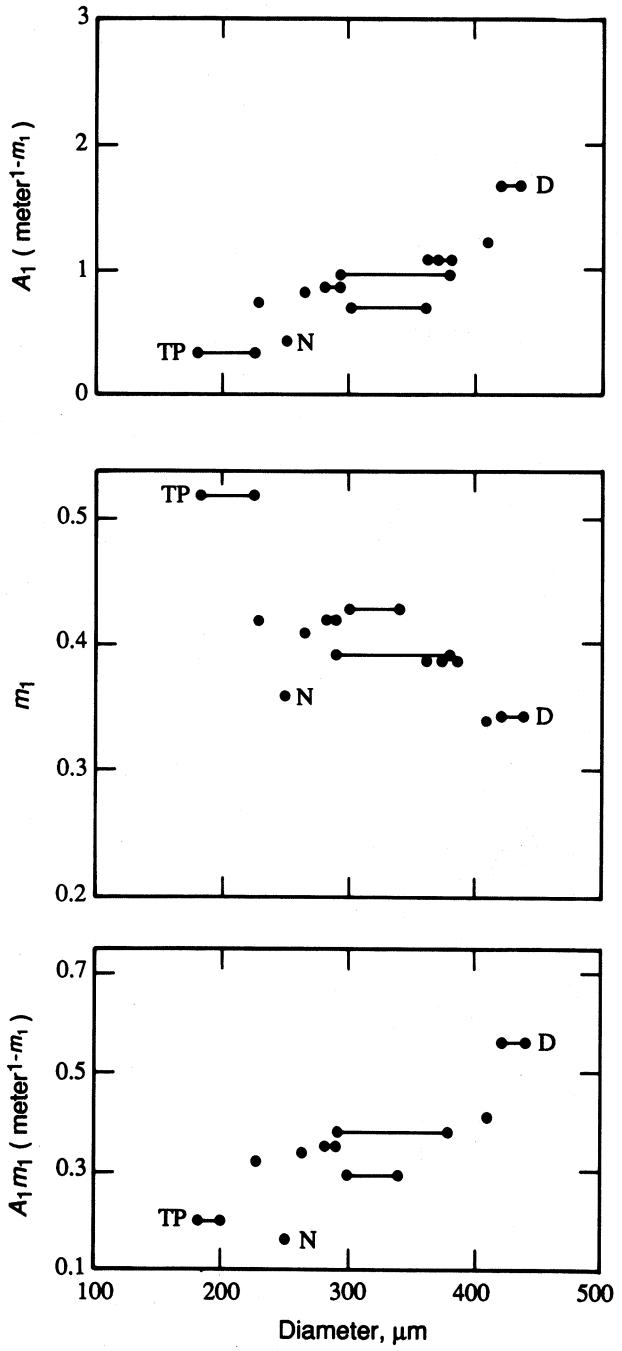

Fig. 11. Fitted bar-berm parameters $h = Ax^m$ versus beach face sand size. Horizontal lines show size range of data in Table 4 for beach face reference level ~1.5 m above MSL. D, N, and TP refer to Duck, Nile delta and Torrey Pines, respectively.

their product A_1m_1 increases from 0.2 to 0.6. With the exception of the Torrey Pines data, m_1 is remarkably stable around a value of 0.4. The Duck data plotted in Figure 11 represent bar-berm data fitted to the first bar (Table 2*b*), and, because of the highly variable distribution of grain size, a composite beach face sample was used [e.g., *Stauble*, 1992]. A similar plot of the shorerise parameters A_2 and m_2 versus the size of sand on the inner reaches of the shorerise (depths 4 and 7 m below MSL) showed no clear trend. However, as noted previously, the increased value of A_2 (i.e., Figure 4, bottom) on range SS3 may, in part, be associated with deposition on the shorerise of coarser sand from the beach face. Generally, the range of sand size on the shorerise is much less than that on the beach face, a situation typical of the world's beaches. For our data, the size range is 90-260 μm at the 4-m depth and 90-135 μm at the 7-m depth.

Although the bar-berm portion of the Torrey Pines profile follows the pattern for the basic data set (Figure 11), the shorerise portion is atypical. It is unusually steep owing to the presence of the fault-controlled, north trending La Jolla Submarine Canyon (Figure 1). The shorerise here slopes at 2.1% (1.2°) from 0 to 20 m depth, compared to the norm for the basic data set of about 0.7% (0.4°). As a consequence, it is not possible for the shorerise slope to decrease to a parabolic shape with depth.

SUMMARY AND CONCLUSIONS

Best fit curves for field data show that the beach profile is well represented by two parabolic curves, matched at the breakpoint-bar (Figure 2). The offshore portion (shorerise) and the onshore portion (bar-berm) are both satisfied by parabolic curves of the form $h = Ax^m$ where both shorerise and bar-berm have values of $A = O(1)$ and $m = O(2/5)$. The matching of these curves at the breakpoint is controlled by changes in the parameters X_1 and X_2 as shown in Figures 2 and 5. The amplification factor A increases with grain size (Figure 11) and varies with season, being generally greater for winter than summer.

The southern California beach profiles attain reproducible equilibrium configurations for summer wave conditions, represented by data for late August to October, and somewhat less reproducible winter conditions, represented by data from March and April. It was found that the changes in seasonal equilibria are manifest by simple, self-similar displacements of the shorerise and bar-berm portions of the curve (Figure 5). The most significant seasonal difference between profiles is that the breakpoint-bar moves offshore and deeper, emphasizing the importance of the breakpoint as a matching area for the two curves.

Comparisons of mean values for the equilibrium summer and winter profiles (Figure 5) give values of seasonal volume changes that are comparable to those obtained in previous studies, i.e., $O(90\ m^3/m)$. Further, since the summer/winter seasonal changes are equal and superimposed on any longer-term shoreline trends, it is suggested that the fixed-form translational profile used in shoreline modeling can be represented by a mean form of the seasonal profiles (Figure 6). The existence and magnitude of the closure interval Z_c of the translational profile are readily determined from the standard deviation of depth change computed for various time intervals within a set of individual profiles (compare Figures 7 and 8).

The spring tidal range (1.8 m) and the occasional higher-than-usual waves act as stretching factors that increase the length of the bar-berm profile, which is generally about 5 times greater than the width of the surf zone. Also, this smoothing effect of tides enhances curve fitting by reducing profile anomalies associated

with the more pronounced longshore bar and trough systems common to tideless seacoasts. However, limited data from the Outer Banks of North Carolina (1-m tides) and from the Nile delta coast (≈ 30-cm tides) indicate that parabolic curves with $A = O(1)$ and $m = O(2/5)$ satisfy these coasts as well. In this regard, it is of interest to compare our findings with those from previous studies where single curves are fit to profile data, usually of more limited range in depth and height. Single-curve studies [e.g., *Bruun*, 1954; *Hayden et al.*, 1975; *Dean*, 1977, 1991; *Larson and Kraus*, 1989] find values of $A \approx 0.15$ and $m = 2/3$. Our data also give these values when fitted from the breakpoint-bar to mean sea level, suggesting that these values are related to the limited range of depth and berm height used in previous studies. In areas where summer waves are consistently small, as along the Nile delta, the small breaker height results in very narrow summer bar-berm profiles. For these special cases a single-fitted curve with iterated best fit origin above the berm provides a fair fit to the summer profile [*Inman et al.*, 1992].

As was mentioned previously, it is not possible to properly fit a parabolic curve to real beach data when the origin falls on the sandy beach profile. This is because parabolic curves are vertical at the origin (vertex) and pass steeply through the point $x = 1$, $h = A$, requiring small values of A to minimize the vertical distortion at the origin. Iteration of our best fit curves always gives the origin of the shorerise at zero MSL, while that for the bar-berm is about one meter above the crest of the berm (Figures 2 and 5). In terms of the mechanics operative over the beach profile, this suggests that shoaling processes over the shorerise are "directed" parabolically toward MSL as a limiting value but are interrupted at the breakpoint. The bar-berm forcing begins at the breakpoint, and the stress asymmetry that increases beach slope continues to increase, seeking the origin as a limit, but reaching a maximum at the crest of the berm where all of the remaining water from the swash percolates into the beach face.

The application of compound parabolic curves to describe equilibrium beach profiles provides a markedly different approach than used in previous studies of this problem. Future study is needed to identify the effect of larger tidal range on compound curve fitting and to resolve the complex problem of curve-fitting to beaches with multiple bars as at Duck, North Carolina, and along the Nile delta.

Acknowledgments. This study was supported by the Office of Naval Research, Coastal Studies, under contract N00014-89-J-1060, and by the Agency for International Development, U.S. State Department, under contract NEB-0158-G-SS-5192, as part of a trilateral United States-Egypt-Israel study, Predictive Model for Shoreline Change along the Nile Littoral Cell. The idea for this study originated during the Coast of California Storm and Tidal Waves Study sponsored by the U.S. Army Corps of Engineers, Los Angeles District, and the profile data for the basic data sets are from the final report of that study [*USACE LAD*, 1991*b*, Appendix B]. Useful insights into this complex problem were provided by Daniel C. Conley, Thomas G. Drake, and Janice Callahan. Manuscript and tables were formatted by Cheryl Bastian Alden and the figures were prepared by Michael P. Clark.

REFERENCES

Aubrey, D. G., D. L. Inman, and C. D. Winant, The statistical prediction of beach changes in southern California, *J. Geophys. Res.*, *85*(C6), 3264–3276, 1980.

Bagnold, R. A., Sand movement by waves: Some small-scale experiments with sand of very low density, *J. Inst. Civ. Eng.*, *27*, 447–469, 1947.

Bagnold, R. A., Mechanics of marine sedimentation, in *The Sea*, vol. 3, *The Earth Beneath the Sea*, edited by M. N. Hill, pp. 507–528, Wiley-Interscience, New York, 1963.

Bailard, J. A., An energetics total load sediment transport model for a plane sloping beach, *J. Geophys. Res.*, *86*(C11), 10,938-10,954, 1981.

Bailard, J. A., and D. L. Inman, An energetics bedload model for a plane sloping beach: Local transport, *J. Geophys. Res.*, *86*(C3), 2035–2043, 1981.

Bascom, W. N., Relationship between sand size and beach face slope, *Eos Trans. AGU*, *32*(6), 866–874, 1951.

Bates, R. L., and J. A. Jackson (Eds.), *Glossary of Geology*, 751 pp., American Geological Institute, Falls Church, Va., 1980.

Bowen, A. J., Simple models of nearshore sedimentation: Beach profiles and longshore bars, in *The Coastline of Canada: Littoral Processes and Shore Morphology*, edited by S. B. McCann, pp. 1–11, Geological Survey of Canada, Ottawa, Ontario, 1980.

Bruun, P., Coast erosion and the development of beach profiles, *Tech. Memo 44*, 79 pp., Beach Erosion Board, U.S. Army Corps of Eng., Washington, D. C., 1954.

Carter, T. G., P. L.-F. Liu, and C. C. Mei, Mass transport by waves and offshore sand bedforms, *J. Waterw. Harbors Coastal Eng. Div.*, Am. Soc. Civ. Eng., *99*(WW2), 165–184, 1973.

Coastal Data Information Program (CDIP), Multi-year report 1975-1991, *SIO Ref. 91-32*, 405 pp., Scripps Inst. of Oceanogr., Univ. of Calif., San Diego, La Jolla, 1992.

Dean, R. G., Equilibrium beach profiles: U.S. Atlantic and Gulf coasts, *Ocean Eng. Rep. 12*, 45 pp. + appendix, Univ. of Del., Newark, 1977.

Dean, R. G., Equilibrium beach profiles: Characteristics and applications, *J. Coastal Res.*, *7*(1), 53–84, 1991.

Dette, H. H., and K. Uliczka, Prototype investigation on time-dependent dune recession and beach erosion, in *Proceedings of Coastal Sediments '87*, pp. 1430–1444, American Society of Civil Engineers, New York, 1987.

Elwany, M. H. S., A. A. Khafagy, D. L. Inman, and A. M. Fanos, Analysis of waves from arrays at Abu Quir Ras El-bar, Egypt, in *Oceanology '88*, *Adv. Underwater Technol.*, vol. 16, pp. 89–97, Graham & Trotman, London, 1988.

Evans, O. F., The low and ball of the eastern shore of Lake Michigan, *J. Geol.*, *48*, 476–511, 1940.

Fenneman, N. M., Development of the profile of equilibrium of the subaqueous shore terrace, *J. Geol.*, *10*, 1–32, 1902.

Hayden, B., W. Felder II, J. Fisher, D. Resio, L. Vincent, and R. Dolan, Systematic variations in inshore bathymetry, *Tech. Rep. 10*, 51 pp., Dep. of Environ. Sci., Univ. of Va., Charlottesville, 1975.

Howd, P. A., and W. A. Birkemeier, Beach and nearshore survey data: 1981–1984, CERC Field Research Facility, *Tech. Rep. CERC-87-9*, 27 pp., Appendices A–F, Coastal Eng. Res. Cent., Waterw. Experiment Sta., U.S. Army Corps of Eng., Vicksburg, Miss., 1987.

Inman, D. L., Areal and seasonal variations in beach and nearshore sediments at La Jolla, California, *Tech. Memo 39*, 134 pp., Beach Erosion Board, U.S. Army Corps of Eng., Washington, D. C., 1953.

Inman, D. L., Accretion and erosion waves on beaches, *Shore & Beach*, *55*(3/4), 61–66, 1987.

Inman, D. L., and R. A. Bagnold, Littoral processes, in *The Sea*, vol. 3, *The Earth Beneath the Sea*, edited by M. N. Hill, pp. 529–553, Wiley-Interscience, New York, 1963.

Inman, D. L., and R. Dolan, The outer banks of North Carolina: Budget of sediment and inlet dynamics along a migrating barrier system, *J. Coastal Res.*, *5*(2), 193–237, 1989.

Inman, D. L., and P. M. Masters, Budget of sediment and prediction of the future state of the coast, in *State of the Coast Report, San Diego Region*, *Coast of California Storm and Tidal Waves Study*, vol. 1 (*Final Report*), chap. 9, p. 1–105, U.S. Army Corps of Engineers, Los Angeles District, Los Angeles, Calif., 1991.

Inman, D. L., M. H. S. Elwany, A. A. Khafagy, and A. Golik, Nile Delta profiles and migrating sand blankets, *Proc. Coastal Eng. Conf., 23rd*, 3273–3284, 1992.

Johnson, D. W., *Shore Processes and Shoreline Development*, 584 pp., John Wiley, New York, 1919.

Kajima, R., T. Shimizu, K. Maruyama, and S. Saito, Experiments of beach

profile change with a large wave flume, *Proc. Coastal Eng. Conf., 18th*, 1385–1404, 1983.

Keulegan, G. H., An experimental study of submarine sand bars, *Tech. Rep. 3*, 40 pp., Beach Erosion Board, U.S. Army Corps of Engin., Washington, D. C., 1948.

Keulegan, G. H., and W. C. Krumbein, Stable configuration of bottom slope in a shallow sea and its bearing on geological processes, *Eos Trans. AGU, 30*(6), 855–861, 1949.

King, C. A. M., and W. W. Williams, The formation and movement of sand bars by wave action, *Geogr. J., 113*, 70–85, 1949.

Kraus, N. C., and S. Harikai, Numerical model of the shoreline change at Oarai Beach, *Coastal Eng., 7*(1), 1–28, 1983.

Kraus, N. C., and M. Larson, Beach profile change measured in the tank for large waves, 1956-1957 and 1962, *Tech. Rep. CERC-88-6*, 39 pp., Appendices A–D, Coastal Eng. Res. Cent., Waterw. Experiment Sta., U.S. Army Corps of Eng., Vicksburg, Miss., 1988.

Larson, M., and N. C. Kraus, SBEACH: Numerical model for simulating storm-induced beach change; empirical foundation and model development, *Tech. Rep. CERC-89-9*, 256 pp., Appendices A–B, Coastal Eng. Res. Cent., Waterw. Experiment Sta., U.S. Army Corps of Eng., Vicksburg, Miss., 1989.

Lau, J., and B. Travis, Slowly varying Stokes waves and submarine longshore bars, *J. Geophys. Res., 78*, 4489–4497, 1973.

LeMéhauté, B., and M. Soldate, Mathematical modeling of shoreline evolution, *Misc. Rep. 77-10*, 56 pp., Coastal Eng. Res. Cent., U.S. Army Corps of Eng., Vicksburg, Miss., 1977.

LeMéhauté, B., and M. Soldate, Mathematical modeling of shoreline evolution, *Proc. Coastal Eng. Conf., 16th*, 1163–1179, 1978.

Nordstrom, C. E., and D. L. Inman, Sand level changes on Torrey Pines Beach, California, *CERC Misc. Pap. 11-75*, 166 pp., Coastal Eng. Res. Cent., U.S. Army Corps of Eng., Vicksburg, Miss., 1975.

O'Reilly, W. C., Modelling the storm waves of January 17-18, 1988, *Shore & Beach, 57*(4), 32–36, 1989.

Roelvink, J. A., and M. J. F. Stive, Bar-generating cross-shore flow mechanisms on a beach, *J. Geophys. Res., 94*(C4), 4785–4800, 1989.

Saville, T., Scale effects in two dimensional beach studies, *Trans. Gen. Meeting of Int. Assoc. of Hydrau. Res., 7th* (1), A3–1 to 10, 1957.

Shepard, F. P., Longshore bars and longshore troughs, *Tech. Memo 15*, 32 pp., Beach Erosion Board, U.S. Army Corps of Eng., Washington, D. C., 1950*a*.

Shepard, F. P., Beach cycles in southern California, *Tech. Memo 20*, 26 pp., Beach Erosion Board, U.S. Army Corps of Eng., Washington, D. C., 1950*b*.

Shepard, F. P., and E. C. LaFond, Sand movements along the Scripps Institution pier, *Am. J. Sci., 238*, 272–285, 1940.

Short, A. D., Offshore bars along the Alaskan arctic coast, *J. Geol., 83*, 209–221, 1975*a*.

Short, A. D., Multiple offshore bars and standing waves, *J. Geophys. Res., 80*(27), 3838–3840, 1975*b*.

Stauble, D. K., Long-term profile and sediment morphodynamics: Field research facility case history, *Tech. Rep. CERC-92-7*, 74 pp. + Appendices A–B, Coastal Eng. Res. Cent., Waterw. Experiment Sta., U.S. Army Corps of Eng., Vicksburg, Miss., 1992.

Strange, R. R., N. E. Graham, and D. R. Cayan, Meterological development of the unusually severe coastal storms during January 16-18, 1988, *Shore Beach, 57*(4), 3–9, 1989.

U.S. Army Corps of Engineers, Los Angeles District (USACE LAD), Sediment sampling, Dana Point to Mexican border (Task 1D, Nov 83-Jan 84), *Coast of California Storm and Tidal Waves Study, CCSTWS 84-5*, Sections 1-3, References, Appendices A–B, Plates 1–7b, Los Angeles, Calif., 1984.

U.S. Army Corps of Engineers, Los Angeles District (USACE LAD), Littoral zone sediments, San Diego Region, Oct 83-Jun 84, *Coast of California Storm and Tidal Waves Study, CCSTWS 85-11*, Sections 1-8, Appendices A–F, Los Angeles, Calif., 1985.

U.S. Army Corps of Engineers, Los Angeles District (USACE LAD), *State of the Coast Report, San Diego Region, Coast of California Storm and Tidal Waves Study*, vol. 1 (*Final Report*), Chap. 1–10, Los Angeles, Calif., 1991*a*.

U.S. Army Corps of Engineers, Los Angeles District (USACE LAD), *State of the Coast Report, San Diego Region, Coast of California Storm and Tidal Waves Study*, vol. 2, Appendices A-I, Los Angeles, Calif., 1991*b*.

Wiegel, R. L., *Oceanographic Engineering*, 532 pp., Prentice-Hall, Englewood Cliffs, N. J., 1964.

Winant, C. D., D. L. Inman, and C. E. Nordstrom, Description of seasonal beach changes using empirical eigenfunctions, *J. Geophys. Res., 80*(15), 1979-1986, 1975.

D. L. Inman, M. H. S. Elwany, and S. A. Jenkins, Center for Coastal Studies, Scripps Institution of Oceanography, La Jolla, CA 92092-0209.

(Received September 18, 1992;
revised April 12, 1993;
accepted April 12, 1993.)